EUROPEAN ORGANIZATION FOR NUCLEAR RESEARCH
CERN - SPS DIVISION

CERN-SPS/ABT/77-13

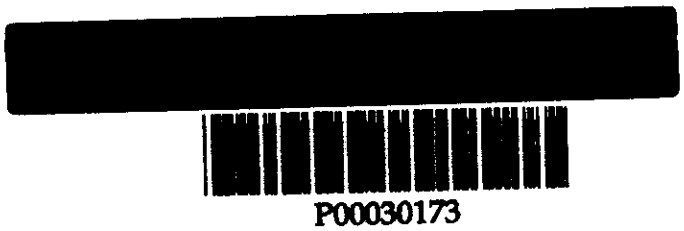

THE STEEL SEPTUM MAGNETS FOR BEAM SPLITTING AT THE CERN SPS

by

L. Evans, A. Ijspeert, B. de Raad, W. Thomi, E. Weisse

Paper presented at the Sixth International Conference on
Magnet Technology
Bratislava 29th August - 2 September 1977

THE STEEL SEPTUM MAGNETS FOR BEAM SPLITTING AT THE CERN SPS

by L. Evans, A. Ijspeert, B. de Raad, W. Thomi, E. Weisse.

CERN, 1211 Meyrin, Geneva, Switzerland

Summary

Each of the two slow-extracted proton beams of the CERN 400 GeV Super Proton Synchrotron (SPS) can be divided into three parts by means of steel-septum magnets for the simultaneous irradiation of up to three production targets[1]. The magnets have radiation-proof coils, integrated vacuum chambers and "plug-in" connections. The paper describes the design of the magnets and gives the results of the magnetic field measurements.

1. - Beam Splitting

The principle of beam splitting is shown in the cross section of the single-septum magnet (fig.1).

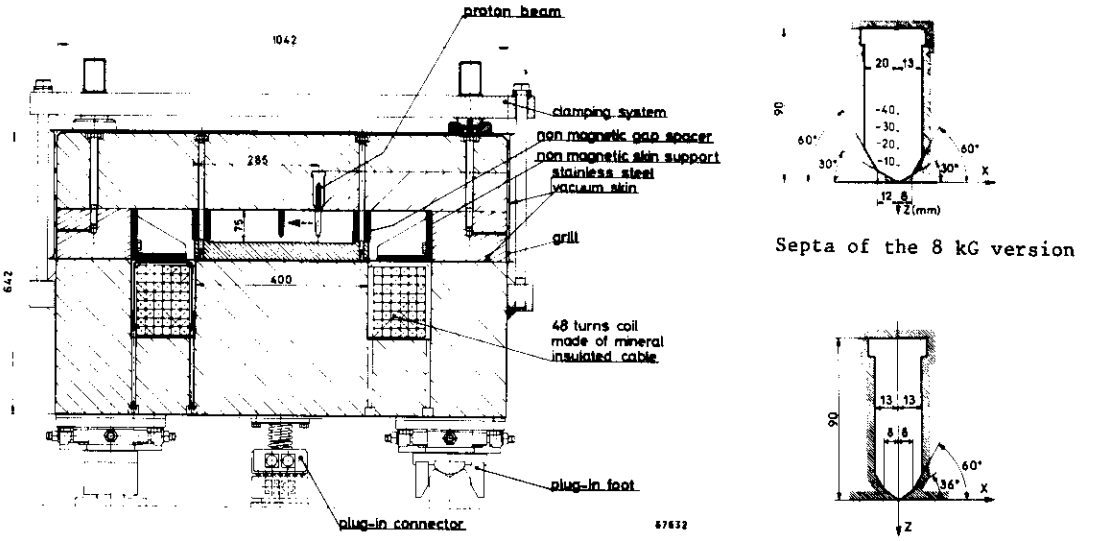

Fig. 1 - Cross section of the single-septum magnet (length 4700 mm, weight 24 tons)

To minimise the beam losses, the septa which separate the hole from the gap are wedge shaped and the beam is blown up to a tall and narrow cross section. A copper collimator in front of the magnet protects the septa against the incident protons. Several beam splits can be made by placing these magnets in cascade. A special version of this magnet type is the double-septum magnet (fig.2) which makes a double beam split. For reasons of beam optics this magnet has a tilted gap.

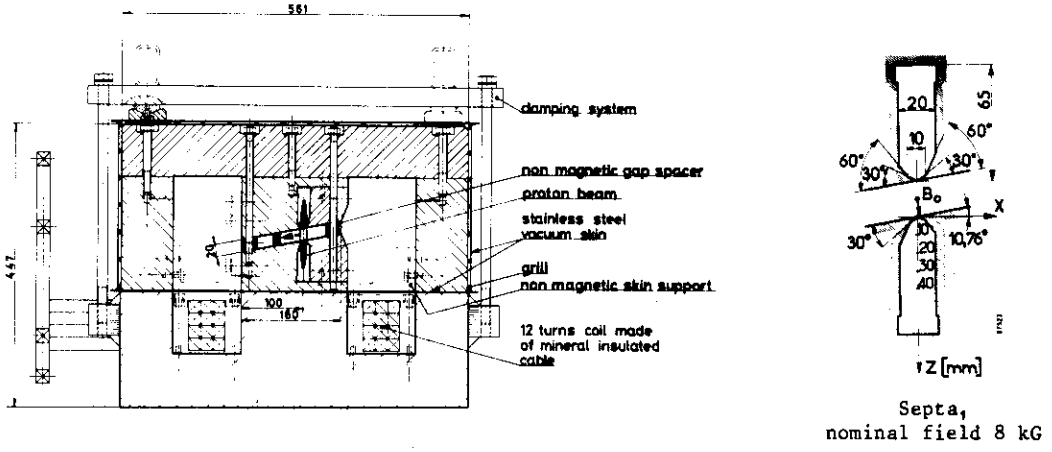

Fig. 2 - Cross section of the double-septum magnet (length 3600 mm, weight 6.2 tons)

2. - The magnetic circuit of the steel-septum magnets

Important factors for the field quality of these magnets are: the shape of the septa, the existence of an iron bridge over the hole, the relation between the iron cross sections left and right of the hole, and the reduction of the fringe fields at the magnet ends.

The shape of the septa must ensure a good field quality in the gap and a minimum stray field level in the hole without causing too much beam loss. Therefore the septum tips have been made as thin as practical for the machining (about 0.1 mm). The wedge angles ϕ have been chosen so that the induction in the wedge, estimated to be $1/\sin\phi$ times the gap field, will be limited to 16 kGauss. The resulting wedge shapes can be seen in figs. 1 and 2 for the 3 versions of magnets used: an 8 kGauss single-septum magnet, a 9.4 kGauss single-septum magnet and an 8 kGauss double-septum magnet. The width of the wedges is defined by the expected proton beam width. Beyond these wedges, the hole widens with a 60° angle for a good clearance around the proton beam.

An iron bridge over the hole is important to allow a transport of magnetic flux over the hole when the latter is not in the centre of the magnet (see fig. 3a, b which have been calculated with the computer program POISSON). Without these iron bridges there would be a much stronger horizontal stray field in the hole(s) and the distribution of the gap field would be more inhomogeneous.

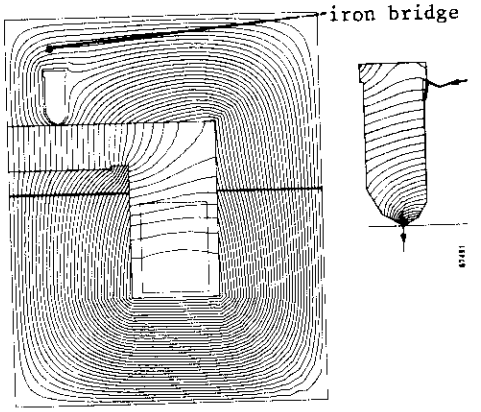

Fig. 3a - Calculated flux pattern of one half of the single-septum magnet at 8 kGauss

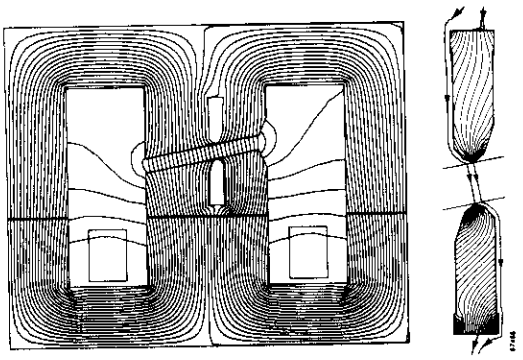

Fig. 3b - Calculated flux pattern of the double-septum magnet at 8 kGauss

The relation between the iron cross section left and right of the hole is important for the same reasons. This lack of symmetry causes the densities of magnetic flux to be different on each side of the hole. This is in particular the case for the pole pieces of the double septum magnet. The tilted pole creates a high flux density in the right hand lower pole piece, partly because of the increased stray flux and partly because of the extra flux which originates from the left hand upper pole piece. As a result, the cross section of this lower pole piece determines to a large extent the field distribution in the gap (fig. 4) and the stray field in the lower hole.

The fringe field at the end of the magnet would strongly disturb the trajectory of the protons traversing the hole. Therefore the upper pole of the single septum magnet has been extended by 220 mm at each magnet end to screen the hole over this distance. In the case of the double septum magnets the effect of the fringe fields has been reduced by mounting mirror plates at 20 mm from each magnet end (fig. 5). Iron bridges over the holes of the mirror plates were necessary to obtain an optimum field distribution.

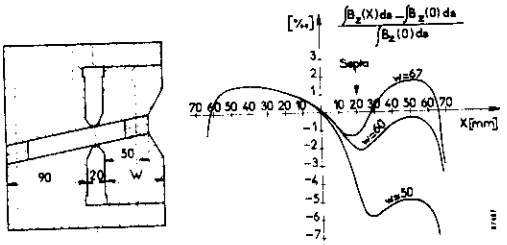

Fig. 4 The influence of the right hand lower pole piece thickness on the field distribution in the gap (measurement on a model of the double-septum magnet at 8 kGauss)

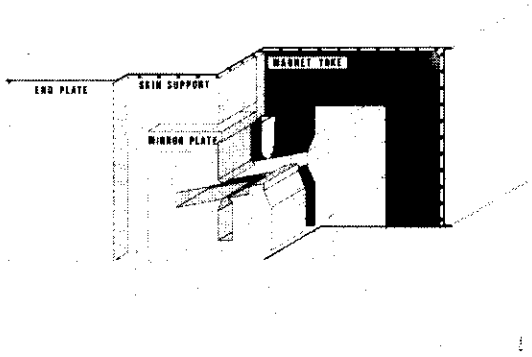

Fig. 5 - View of the mirror plate (double-septum magnet)

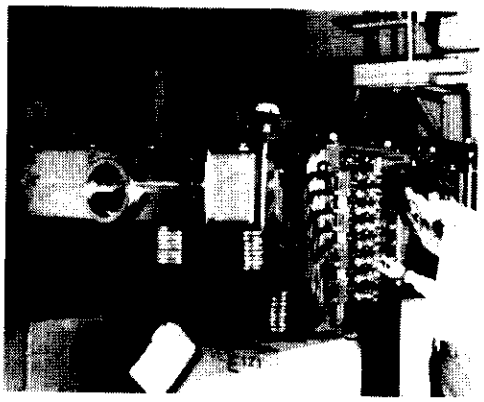

Fig. 6 - View on the coil end (single septum magnet)

3. - Design of the magnets

The magnet core has been made from precisely ground pieces of solid steel, bolted together*. Ground aluminium gap spacers guarantee a precise gap height. The septum straightness, pole flatness, pole parallelism and nominal gap height must be excellent to minimize the proton losses from the part of the beam which scrapes along the pole. They are all precise to within 0.04 mm.

The vacuum skin, a 1 mm thick stainless steel sheet, is welded around the upper half core to form an integrated vacuum chamber. A stainless steel grill is pinched between the skin and the yoke to improve the conductance for vacuum pumping. At each end, the skin is welded on a stainless steel end plate equipped with a vacuum flange. Aluminium skin supporting pieces are mounted at the places where the skin is not supported by the magnet yoke against atmospheric pressure.

The coils (fig. 6) have been wound ** from 0.75" square hollow mineral insulated cable[2] because of the high radiation level (up to 10^{11} rad/year) during operation. At the coil ends the hygroscopic magnesium-oxide powder is sealed against the penetration of air humidity by ceramic seals (fig. 7). In general, to avoid radiation damage, all the insulators are ceramic and the water hoses and seals are metallic.

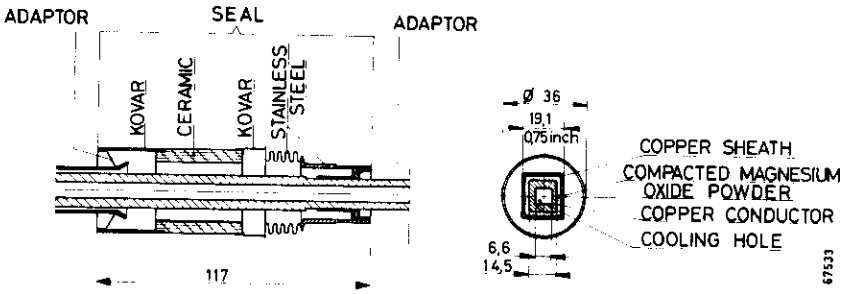

Fig. 7 - Cross section of the 0.75" mineral insulated cable and the powder seal

The feet, hydraulic and electrical connections are of a plug-in type to allow a quick exchange of magnets (see fig.1)***. They are mounted under the magnets and adjusted in the Laboratory to make all the magnets identical and remotely exchangeable. When a magnet is installed, the feet first centre the magnet roughly, then the connectors engage and finally the feet centre precisely on the wedge shaped supports.

4. - Magnetic field measurements

The field in the magnet gap has been measured with a moving measuring-coil assembly composed of 3 consecutive coil elements with a cross section of 10 mm x 10 mm. The stray field in the holes has been measured with two Hall probes to measure the vertical and the horizontal field components.

---

*)The cores have been made by VOEST, Austria.
**)The coils have been wound by SEGCEM, France. The cable is made by PYROTENAX, Canada.
***)They have been developed by M. Ellefsplass, SME Group, SPS Division, CERN.

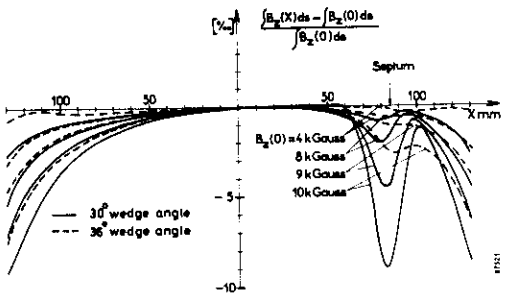

Fig. 8a - The distribution of the integrated field of the single-septum magnet (measured at 8.5 mm from the upper pole).

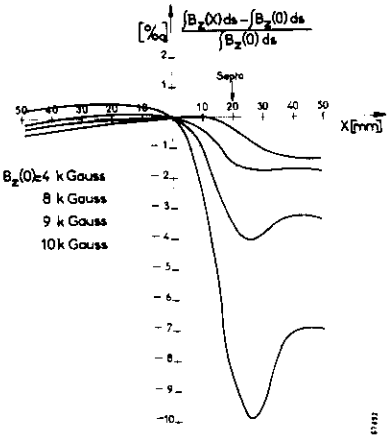

Fig. 8b - The distribution of the integrated field of the double-septum magnet (measured in the median plane of the gap)

At different gap fields, height Z = 1mm

Nom. field [k Gauss]	$\int B_z\,ds$ Gauss m	B_z inside [Gauss]	$\int B_x\,ds$ Gauss m	B_x inside [Gauss]
4	30	3	+13	+3
8	240	35	-170	-35
9	320	90	-290	-60
10	1030	200	-525	-110

At different heights, gap field = 8 k Gauss

Height Z [mm]	$\int B_z\,ds$ Gauss m	B_z inside [Gauss]	$\int B_x\,ds$ Gauss m	B_x inside [Gauss]
-1	240	35	-170	-35
-5	170	20	-100	-20
-10	130	13	-80	-17
-20	80	4	-35	-8
-40	50	0	-30	-7

a) single-septum magnet 30° wedge angle

At different gap fields, height Z = -1mm

Nom. field [k Gauss]	$\int B_z\,ds$ Gauss m	B_z inside [Gauss]	$\int B_x\,ds$ Gauss m	B_x inside [Gauss]
4	40	1	40	+9
8	90	4	-25	-4
9	120	9	-50	-9
10	240	35	-75	-14
11	640	125	-120	-22

b) single-septum magnet 36° wedge angle

At different gap fields, height Z = 1mm

Nom. field kGauss	$\int B_z\,ds$ Gauss m	B_z inside Gauss	$\int B_x\,ds$ Gauss m	B_x inside Gauss
4	12	2	-34	-10
8	100	12	-100	-30
9	250	45	-140	-37
10	620	135	-290	-70

At different heights, gap field = 8 k Gauss

Height Z mm	$\int B_z\,ds$ Gauss m	B_z inside Gauss	$\int B_x\,ds$ Gauss m	B_x inside Gauss
1	100	12	-100	-30
5	35	3	-88	-23
10	20	2	-70	-18
20	8	2	-60	-15
40	0	13	-42	-12

c) double-septum magnet

Fig. 9 - The stray field measured in the hole (see for the co-ordinates figs. 1 & 2)

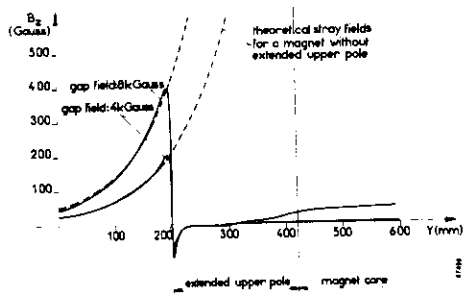

Fig. 10a - The fringe field in front of the hole measured at 1 mm above the septa : single-septum magnet

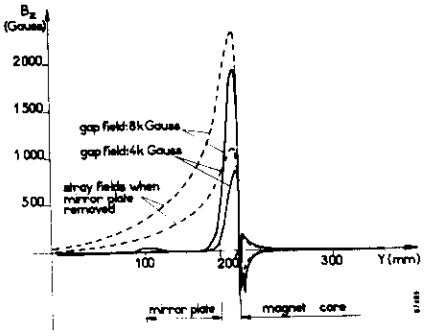

Fig. 10b - The fringe field in front of the hole measured at 1 mm above the septa : double-septum magnet

The distribution of the integrated field in the gap is shown in fig. 8a,b, measured at 8.5 mm from the upper pole of the single septum magnet (at larger distance, the field perturbation decreases rapidly) and in the median plane of the gap of the double-septum magnet.

The curves shown are averages of two measurements: one where the field was increased from zero to the desired value (case a) and a second where the field was decreased from 11 kGauss to the desired value (case b). Because of the remanence of the iron, the amplitude of the disturbance under the septa of the single septum magnet is about 6 Gauss larger in case a than in case b (measured from peak to peak) at 4 and 8 kGauss. For the same reason, the field drop at

positive x in the double-septum magnet is about 4 Gauss smaller in case a than in case b at all the measured field levels.

The stray field in the hole and the integrated stray field felt by the particles traversing the hole (fringe field included) are listed in fig. 9 as averages of the measurements of case a and case b. The shape of the fringe fields is shown in fig. 10a, b.

5. - Estimation of the disturbance of the gap field caused by the septa

To understand the influence of the different septum parameters on the field disturbance it is possible to make a simplified analytical calculation[3] for a symmetric steel septum magnet. Along the central flux line (fig. 11) one can estimate the integral of Hdl of the field disturbance to equal the loss of the integral of Hdl in the septum. Writing (ΔB_z)av for the average field disturbance over the height of the gap at x = o and $(\text{Bseptum}/\mu r)_{av}$ for the average field along this flux line in the septum :

$$(\Delta B_z)_{av} . b = (\text{Bseptum})/\mu r)_{av} . (x_1/\cos\phi) \qquad (1)$$

The induction in the septa can be estimated to be

$$\text{Bseptum} = \text{Bgap}/\sin\phi \qquad (2)$$

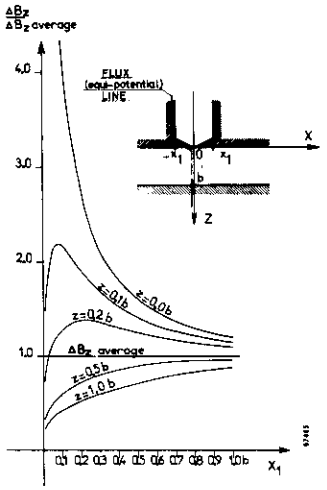

Fig. 11 - The field dip under the septa B_z at x = o, calculated at different heights z as a function of the septum width x_1

(This estimation is rather speculative as Bseptum and its direction are not necessarily constant, but it gives a useful approximation). This yields $(\Delta B_z)_{av}$. The distribution of ΔB_z along the z-axis can be approximated to be :

$$\frac{\Delta B_z(z)}{\Delta B_z(o)} = +1 - \frac{2}{\pi} \arctan \frac{\sin \frac{\pi}{2b} z}{\sinh \frac{\pi}{2b} x_1} \qquad (\text{where } 0 \leq z \leq b) \qquad (3)$$

where b represents the gap height of the single septum magnet or half the gap height of the double-septum magnet and x_1 represents the septum width.

Fig. 11 gives the ratio $\Delta B_z/(\Delta B_z)_{av}$ as calculated with this formula.

Comparison of the estimated field dip with the measured results shows a precision within a factor 2 for field disturbances of at least $1^0/oo$ with the exception that for the single-septum magnets the field disturbance disappears quicker than expected for increasing z.

6. - Conclusion

The steel septum magnets provide a good means for beam splitting. A satisfactory field quality and a sufficiently low stray field in the hole(s) have been obtained. The magnets which operate since the end of 1976 perform well and reliably. Another group of magnets will come into operation early 1978.

References

1. L. Evans, A. Hilaire, A. Ijspeert, B. de Raad, N. Siegel, E. Weisse. The external proton beam lines and the splitter system of the CERN SPS. Proc. of the Particle Accelerator Conference, Chicago 1977.

2. A. Harvey, Proc. of the 4th Int. Conf. on Magnet Technology, Brookhaven 1972, page 456.

3. A. Ijspeert, Calculation of the field disturbance caused by steel septa, SPS/ABT/AI/Int.77-3, to be published.